

Synthesis and QSAR of new azomethine derivatives as agents for the treatment of Alzheimer's disease

Chiriapkin A.S., Kodonidi I.P., Pozdnyakov D.I., Zolotykh D.S.

Pyatigorsk medical and pharmaceutical Institute-branch of Volgograd state medical University of the Ministry of health of the Russian Federation (Pyatigorsk, Russia (357532, Pyatigorsk, av. Kalinina 11).

Abstract

Alzheimer's disease is a chronic neurodegenerative disease with a high risk of social maladaptation. The number of cases of the disease is constantly increasing, which, with a shortage of effective drugs for the treatment and prevention of this disease, makes it urgent to develop new medicines for the treatment of Alzheimer's disease. In this regard, the aim of the study was to synthesize, evaluate anti-amyloid and anticholinesterase activity, as well as to study the structure-activity relationship of new azomethine derivatives. As a result, it was found that the compounds 3d; 3e; 3f; 3m; 3n and 3o have the highest anticholinesterase activity, for which the IC₅₀ index was comparable to donepezil. Pronounced anti-amyloid activity was demonstrated by 3g; 3j; 3k and 3p compounds, comparable in activity level with GV-971. The evaluation of the structure-activity relationship showed that the most reliable model for predicting the amyloid-inhibitory properties of azomethine derivatives was obtained using Artificial neural network with values $R^2 = 0.9926$ and $Q^2 = 0.9923$, at the same time anticholinesterase properties $R^2 = 0.9073$ and $Q^2 = 0.7688$.

Key words: Alzheimer's disease, azomethine derivatives, anticholinesterase action, QSAR, medical chemistry

Introduction

Alzheimer's disease (AD) is the most common neurodegenerative disease and a terminal form of dementia. At the moment, more than 50 million people suffer from AD. According to various forecasts, the incidence of AD in the coming years will increase exponentially and by 2050 will amount to more than 152 million people. In addition to the high epidemiological and social role for AD, it significantly affects the economic component of the healthcare system: more than 500 billion US dollars are spent annually on the necessary drug provision and maintenance of an adequate standard of living for patients with AD [1]. Nowadays, there are no clinically effective strategies for the treatment of AD. As a rule, the therapy is limited to the elimination of symptoms of cholinergic deficiency, which is achieved through the targeted use of anticholinesterase drugs. Also, the existing methods of treating AD include the suppression of glutamate-dependent excitotoxic reactions through the use of NMDA receptor blockers - adamantane derivatives [2]. Currently being developed drugs for the treatment of AD are gradually moving away from the principles of symptomatic therapy and directly affect the pathogenesis of the disease, an important aspect of which is the accumulation of β -amyloid fragments ($A\beta$) [3]. $A\beta$ is a product of the catalytic degradation of the amyloid precursor protein with the participation of secretase group enzymes (β -secretase and γ -secretase) and is the main cause of the formation of senile plaques. Stable fragments of $A\beta_{40-42}$ can accumulate in brain structures such as the hippocampus, amygdala or cerebral cortex, causing neurotoxic reactions that are accompanied by degeneration of axons and dendrites, synaptic dysfunction and cognitive deficits [4]. Given the leading role of amyloidogenesis in the pathogenesis of AD, it is not surprising that this pathogenetic aspect of the disease has become one of the promising pharmacotherapeutic targets. Anti-amyloid therapy includes the use of promising β -secretase and γ -secretase modulators, α -secretase activators, direct inhibitors of $A\beta$ aggregation and monoclonal antibodies to $A\beta$ fragments [5]. Many of these drugs are successfully undergoing phase III clinical trials. However, the development of new anti-amyloid drugs does not lose its scientific and

practical value and is an actual direction of medical chemistry and pharmacology.

It is worth noting that azomethine derivatives of 2-amino-4,5,6,7-tetrahydro-1-benzothiophene-3-carboxamide are often not isolated as intermediate products of the reaction of obtaining their thiophenopyrimidines [6-8], and therefore that is a poorly studied class of organic compounds. A method is known for obtaining these azomethines by reacting 2-amino-4,5,6,7-tetrahydro-1-benzothiophene-3-carboxamide with the corresponding aldehydes in a boiling toluene medium [9]. Azomethine derivatives of this chemical group are known to inhibit protein kinase G from *Mycobacterium tuberculosis* [10] and fibroblast growth factor [11]. The azomethine derivatives of 2-amino-4,5,6,7-tetrahydro-1-benzothiophene-3-carboxamide obtained using triethyl orthoformate and 4-chlorobenzaldehyde have antibacterial properties against *Staphylococcus aureus*, *Bacillus subtilis*, *Pseudomonas aeruginosa* and *Escherichia coli* [12]. Also, for some azomethine derivatives, the presence of neurotropic activity, in particular antidepressant [13] and anticonvulsant properties has been described [14], this opens up certain prospects for the creation of neuroactive compounds, including those affecting the pathogenesis of AD, based on azomethine scaffold.

Based on the structural analysis of a number of AChE inhibitors, common structural fragments were identified, presumably having an important role in inhibiting the enzyme. As such a significant structural feature, a carbomatic fragment contained in neostigmine and physostigmine preparations can be considered. Another pharmacophore fragment is the presence of hydroxyphenyl and/or methoxyphenyl substructures included in the structure of many AChE inhibitors. As an example, Figure 1 shows the structural formulas of Donepezil (medicine) [15], Sophorflavexenol [16], Epiberberine [17], Scopoletin [18], Jatrorrhizine [18] and Dehydronuciferine [19]. In the structure of these compounds, there are hydroxy and/or methoxy groups in the aromatic part of the molecules. It is also possible to isolate a similar fragment with a nitrogen atom, which is part of a heterocyclic system. For Donepezil and Epiberberine, a five-membered cycle can be noted in

the structure. Epiberberine has two oxygen atoms in this cycle. We propose to use as a scaffold a skeleton of azomethine derivatives of 2-amino-4,5,6,7-tetrahydro-1-benzothiophene-3-carboxamide. The aryl fragment containing the hydroxyphenyl and/or methoxyphenyl fragment of the compound is introduced as a result of interaction with the corresponding aldehydes and has high variability. A fragment with a nitrogen atom is presented here in aliphatic part in the form of an azomethine bond, which, as well as a hydroxyphenyl and/or methoxyphenyl fragment, can increase the probability of these structures to inhibit the enzyme. As in Donepezil and Epiberberine, a five-membered cycle is present in the structure of the proposed compounds, which is represented in azomethine derivatives of 2-amino-4,5,6,7-tetrahydro-1-benzothiophene-3-carboxamide in the form of a thiophene heterocycle. As a result of the logical-structural approach to the analysis of AChE inhibitors, azomethine derivatives of 2-amino-4,5,6,7-tetrahydro-1-benzothiophene-3-carboxamide may be effective as AChE inhibitors.

Materials and methods

Chemistry

All chemicals were acquired from Sigma-Aldrich (SigmaAldrich, St. Louis, MO, USA), Carl Roth (Carl Roth, Karlsruhe, Germany) and Merck Chemicals (MerckKGaA, Darmstadt, Germany). Melting points (m.p.) were recorded using the PMP-M1 melting point apparatus (Himlaborpribor, Klin, Russia). All reactions were monitored by thin-layer chromatography (TLC) using silica gel 60 F254 TLC plates (Merck, Darmstadt, Germany). Spectroscopic data were registered with the following instruments: IR, IR-Fourier FSM 1201 spectrophotometer (Spectrum, Moscow, Russia); UV, SF-2000 device (Spectrum, Moscow, Russia); ¹H NMR and ¹³C NMR, Bruker Avance III 400 MHz spectrometer (Bruker, Germany) in DMSO-d₆ using tetramethylsilane as the internal standard. Coupling constant (J) values are measured in hertz (Hz) and spin multiples are given as s (singlet), d (double), t (triplet), q (quartet), m (multiplet).

General procedure for synthesis of azomethine derivatives of 2-amino-4,5,6,7-tetrahydro-1-benzothiophene-3-carboxamide (3a-3s)

0.01 mol (1.92 g) of compound 1 and the equimolar amount of the corresponding aldehyde

(2) were dissolved by heating in a minimum amount of ethanol. Then the solutions were combined and the reaction was carried out until a precipitate was formed. It took about 10-30 minutes. The precipitate was filtered and purified by recrystallization from ethanol. Compounds 3a-3j, 3p, 3q were obtained earlier [20].

Molecular modeling

The target of molecular docking is human acetylcholinesterase. This enzyme was studied by X-ray diffraction analysis and its three-dimensional model are given in RCSB Protein Data Bank database (rcsb.org) with the identification number 2EY7 [21]. The virtual complex of 2EY7 contains its inhibitor - Donepezil, which allows for a qualitative assessment of the conformational complex of the simulated compounds with the enzyme obtained in silico. It is also possible to propose a mechanism for the amino acid interaction of the ligand with the active site of AChE in the course of a computational experiment with a high degree of probability. The three-dimensional structures of the studied compounds were constructed in the HyperChem 8.0.4 program and then geometrically optimized by the molecular mechanics method using the MM+ method [22]. The final geometry optimization of the virtual structures was calculated in the ORCA 4.1 program using the density functional theory (UB3LYP) method and the 6-311G** basis set. The conversion of the hin format to the pdb required for molecular modeling was carried out in the Open Babel 2.4.1 program. The docking study was performed using the Autodock 4.0 program [23]. Molecular modeling was performed subject to the conformational flexibility of the ligands. The charges of all the atoms of the simulated system are calculated by the Gasteiger algorithm. The area of the computational experiment is a cube. The center of a box is located: x = -13.98; y = -43.97; z = 27.89. The spacing is 0.375 angstrom. The number of points in x-, y- and z-dimension are 46. The program was set to search for 200 energetically favorable conformations of the ligand-enzyme complex formation using the Lamarckian GA 4.2 scoring function for calculating the energy of the ligand-enzyme interaction.

Root mean square deviation (RMSD) for validation docking was done using the location of the Donepezil at the complex 2EY7 (X-ray diffraction analysis) and its location according to the molecular

docking data. Calculating RMSD was made according to the equation:

$$MSD = \sqrt{\frac{1}{N} \sum_{i=1}^N r_i^2}$$

where RMSD is a root mean square deviation, Å; N is a number of atoms; r_i is a distance between the corresponding atoms i , Å.

Pharmacological study

Evaluation of anti-amyloid activity in vitro

The aggregation process of amyloid particles was evaluated in the reaction of the interaction of A β with congo red. 25 μ l of a solution of the test compounds in dimethyl sulfoxide (the final concentration is 20 mg / ml, GV-971 in a similar concentration was used as a referent compound) was mixed with 225 μ l of a 20 mM solution of congo red in phosphate buffer solution. The resulting mixture was incubated at room temperature. Then the absorbance of the samples was recorded at wavelength 540 nm and 405 nm. after nine days of incubation. The number of aggregates A β was calculated by the formula:

$$A\beta = \frac{A540}{4780} - \frac{A405}{6380} - A405BL/8620$$

where

A405BL - absorbance of the congo red solution at a wavelength of 405 nm;

A540 and A405 - absorbance of the solution containing the test substances at a wavelength of 540 nm and 405 nm, respectively.

The fragment A β 1-40 was obtained from Sigma-Aldrich (Germany). GV-971 was provided by Hunan warrant pharm. (China). The difference between the compounds was evaluated by the ANOVA method with the Tukey post-test [24].

Evaluation of anticholinesterase activity in vitro

The activity of acetylcholinesterase was determined by the modified Ellman method. The analyzed medium contained 20 ml of acetylcholinesterase solution (3.2 U / l), 25 ml of a solution of the test compounds in various concentrations (30 mg/ml, 15 mg/ml, 7.5 mg/ml, 3.75 mg/ml and 1.875 mg/ml) and a potassium-phosphate buffer solution in a volume of up to 300 ml. Donepezil (KRKA, Slovenia) in similar concentrations

was used as a reference substance. The mixture was incubated for 5 minutes. The reaction was started by adding acetylcholine chloride (25 μ l, 0.02 M solution) and 5.5' - dithiobis-2-nitrobenzoic acid ((25 μ l, 0.02 M solution). The absorbance of the mixture was recorded after 5 minutes at 412 nm. using the Infifnte F50 microplate reader (Tecan, Austria). The tests were performed in a triplet version. IC₅₀ (mg / ml) was calculated by probit analysis. The data is presented in the form of $M \pm SEM$ (mean \pm standard error of the mean). Statistical differences were evaluated at a significance level of $p < 0.05$ by the ANOVA method with post-processing by Tukey [25].

QSAR-model

Molecular descriptors of different classes were calculated using T.E.S.T. software. Further descriptor selection, constructing of prediction models and cross-validation of models was realized with the help of trial version of Molegro Data Modeller 7 [23].

Results

Synthesis

As shown in Figure 2 2-amino-4,5,6,7-tetrahydro-1-benzothiophene-3-carboxamide 1 and aldehydes 2 were refluxed in ethanol to obtain azomethine derivatives of 2-amino-4,5,6,7-tetrahydro-1-benzothiophene-3-carboxamide 3. The reactions were performed in ethanol as a green solvent. The method showed to be facile, fast, and efficient, and gave the products in high yields. The compounds were characterized by nuclear magnetic resonance and infrared spectroscopy.

2-[(3,5-ditert-butyl-4-hydroxyphenyl)methyleneamino]-4,5,6,7-tetrahydrobenzothiophene-3-carboxamide (3k)

The yellow crystals were obtained. Yield: 85%. M.p.: 261-264°C. UV spectrum (ethanol), λ_{max} , nm: 206, 250, 313, 393. IR spectrum (KBr). ν , cm⁻¹: 3454 (OH, stretching), 3228 (NH), 2947 (Csp³-H), 1641 (C=O), 1593 (N=CH). ¹H NMR spectrum (400 MHz, DMSO-d₆), δ , ppm: 1.42 (s, 18H, CH₃), 1.83 – 1.63 (1.68, 1.70, 1.75, 1.76, 1.77, m, 4H, CH₂), 2.66 (2.65, 2.67, 2.68, t, J = 6.4 Hz, 2H, CH₂), 2.75 (2.75, 2.76, 2.78, t, J = 6.0 Hz, 2H, CH₂), 7.49 (7.49, 7.50, d, J = 3.0 Hz, 1H, ArH), 7.72 (d, J = 1.8 Hz, 2H, ArH, NH), 7.80 (7.80, 7.81, d, J = 1.7 Hz, 1H, NH), 8.27 (s, 1H, OH), 8.45 (s, 1H, C=NH). ¹³C NMR spectrum (100,6 MHz, DMSO-d₆), δ , ppm: 22.64, 23.07, 25.40, 26.56,

30.47, 34.98, 126.66, 126.90, 128.24, 130.35, 136.32, 139.49, 152.00, 158.53, 158.66, 165.56.

2-[(2-hydroxy-5-nitro-phenyl)methyleneamino]-4,5,6,7-tetrahydrobenzothiophene-3-carboxamide (3l)

The yellow amorphous compound was obtained. Yield: 88%. M.p.: 219-221°C. UV spectrum (ethanol), λ_{\max} , nm: 204, 308, 393. IR spectrum (KBr). ν , cm⁻¹: 3372 (OH, stretching), 3188 (NH), 2932 (Csp³-H), 1646 (C=O), 1601 (N=CH). ¹H NMR spectrum (400 MHz, DMSO-d₆), δ , ppm: 1.85 – 1.68 (1.71, 1.73, 1.77, 1.78, 1.80, 1.181, m, 4H, CH₂), 2.60 (2.59, 2.61, 2.62, t, J = 6.2 Hz, 2H, CH₂), 2.72 (2.71, 2.72, 2.74, t, J = 6.2 Hz, 2H, CH₂), 7.13 (7.12, 7.14, d, J = 9.2 Hz, 1H, ArH), 7.63 (s, 1H, ArH), 7.89 (s, 1H, ArH), 8.24 (8.23, 8.24, 8.25, 8.26, dd, J = 9.1, 2.9 Hz, 1H, NH), 8.70 (8.69, 8.70, d, J = 2.9 Hz, 1H, NH), 8.79 (s, 1H, C=NH), 12.99 (s, 1H, OH).

2-[5-bromo-2-hydroxy-3-methoxy-phenyl)methyleneamino]-4,5,6,7-tetrahydrobenzothiophene-3-carboxamide (3m)

The yellow amorphous compound was obtained. Yield: 95%. M.p.: 224-226°C. UV spectrum (ethanol), λ_{\max} , nm: 203, 227, 294, 394. IR spectrum (KBr). ν , cm⁻¹: 3402 (OH, stretching), 3296 (NH), 3199 (NH), 2931 (Csp³-H), 1657 (C=O), 1597 (N=CH). ¹H NMR spectrum (400 MHz, DMSO-d₆), δ , ppm: 1.84 – 1.68 (1.70, 1.71, 1.73, 1.77, 1.79, 1.80, 1.82, m, 4H, CH₂), 2.60 (2.58, 2.71, 2.72, t, J = 6.0 Hz, 2H, CH₂), 2.71 (2.69, 2.71, 2.72, t, J = 6.2 Hz, 2H, CH₂), 3.85 (s, 3H, CH₃), 7.24 (7.24, 7.24, d, J = 2.3 Hz, 1H, ArH), 7.57 – 7.47 (7.49, 7.40, 7.53, 7.55, m, 2H, ArH, NH), 7.82 (s, 1H, NH), 8.62 (s, 1H, N=CH), 11.72 (s, 1H, OH). ¹³C NMR spectrum (100,6 MHz, DMSO-d₆), δ , ppm: 22.41, 23.11, 25.19, 25.35, 56.83, 110.37, 117.99, 121.75, 124.08, 132.77, 133.18, 134.88, 147.33, 148.97, 149.64, 155.39, 165.75.

2-[5-bromo-2-hydroxy-3-methyl-phenyl)methyleneamino]-4,5,6,7-tetrahydrobenzothiophene-3-carboxamide (3n)

The yellow amorphous compound was obtained. Yield: 93%. M.p.: 221-223°C. UV spectrum (ethanol), λ_{\max} , nm: 203, 218, 292, 394. IR spectrum (KBr). ν , cm⁻¹: 3462 (OH, stretching), 3354 (NH), 2931 (Csp³-H), 1676 (C=O), 1593 (N=CH). ¹H NMR spectrum (400 MHz, DMSO-d₆), δ , ppm: 1.70-1.82 (1.71, 1.72, 1.73, 1.74, 1.75, 1.77, 1.78, 1.89, 1.81, m, 4H, CH₂), 2.27 (s, 3H, CH₃), 2.56 (2.54, 2.55, 2.57, t, J = 6.0 Hz, 2H, CH₂), 2.76 – 2.68 (2.70, 2.72, 2.73, t, J = 6.3 Hz, 2H, CH₂),

7.48 (7.48, 7.48, d, J = 2.1 Hz, 1H, ArH), 7.54 (7.53, 7.54, d, J = 2.1 Hz, 1H, ArH), 7.62 (s, 1H, NH), 7.79 (s, 1H, NH), 8.57 (s, 1H, C=NH), 12.91 (s, 1H, OH). ¹³C NMR spectrum (100,6 MHz, DMSO-d₆), δ , ppm: 20.01, 22.36, 23.14, 24.78, 25.32, 109.97, 120.46, 129.97, 132.41, 133.19, 134.25, 134.28, 136.70, 145.56, 154.20, 157.60, 165.88.

2-[(3,5-dibromo-2-hydroxy-phenyl)methyleneamino]-4,5,6,7-tetrahydrobenzothiophene-3-carboxamide (3o)

The yellow amorphous compound was obtained. Yield: 92%. M.p.: 227-230°C. UV spectrum (ethanol), λ_{\max} , nm: 203, 222, 294, 394. IR spectrum (KBr). ν , cm⁻¹: 3429 (OH, stretching), 3292 (NH), 3192 (NH), 2931 (Csp³-H), 1653 (C=O), 1604 (N=CH). ¹H NMR spectrum (400 MHz, DMSO-d₆), δ , ppm: 1.84 – 1.68 (1.71, 1.72, 1.73, 1.74, 1.75, 1.76, 1.78, 1.80, 1.81, m, 4H, CH₂), 2.56 (2.54, 2.56, 2.57, t, J = 6.1 Hz, 2H, CH₂), 2.71 (2.71, 2.72, 2.74, t, J = 5.8 Hz, 2H, CH₂), 7.65 (d, J = 2.1 Hz, 1H, ArH), 7.81 (s, 1H, ArH), 7.91 (7.89, 7.89, 7.93, 7.93, dd, J = 15.4, 2.4 Hz, 2H, NH), 8.62 (s, 1H, C=NH), 13.28 (s, 1H, OH). ¹³C NMR spectrum (100,6 MHz, DMSO-d₆), δ , ppm: 22.32, 23.10, 24.76, 25.35, 110.64, 111.55, 122.14, 134.09, 134.16, 134.36, 134.96, 137.42, 145.04, 155.76, 156.36, 165.76.

2-[(5-iodo-2-furyl)methyleneamino]-4,5,6,7-tetrahydrobenzothiophene-3-carboxamide (3r)

The brown crystals were obtained. Yield: 94%. M.p.: 139-142°C. UV spectrum (ethanol), λ_{\max} , nm: 206, 323, 407. IR spectrum (KBr). ν , cm⁻¹: 3394 (NH), 3244 (NH), 2943 (Csp³-H), 1657 (C=O), 1630 (N=CH). ¹H NMR spectrum (400 MHz, DMSO-d₆), δ , ppm: 1.81 – 1.64 (1.67, 1.68, 1.69, 1.69, 1.70, 1.71, 1.72, 1.74, 1.75, 1.77, 1.78, m, 4H, CH₂), 2.68 (2.66, 2.68, 2.69, t, J = 6.0 Hz, 2H, CH₂), 2.74 (2.72, 2.74, 2.75, t, J = 6.1 Hz, 2H, CH₂), 6.99 (6.98, 6.99, d, J = 3.5 Hz, 1H, ArH), 7.16 (7.15, 7.16, d, J = 3.5 Hz, 1H, ArH), 7.41 (s, 1H, NH), 8.16 (s, 1H, NH), 8.20 (s, 1H, N=CH). ¹³C NMR spectrum (100,6 MHz, DMSO-d₆), δ , ppm: 22.54, 23.01, 25.45, 26.36, 101.02, 122.07, 123.88, 130.08, 131.81, 136.50, 143.28, 150.61, 156.21, 165.38.

2-[[5-(4-nitrophenyl)-2-furyl]methyleneamino]-4,5,6,7-tetrahydrobenzothiophene-3-carboxamide (3s)

The maroon crystals were obtained. Yield: 91%. M.p.: 205-208°C. UV spectrum (ethanol), λ_{\max} , nm: 204, 346, 434. IR spectrum (KBr). ν , cm⁻¹: 3442 (NH, stretching), 2928 (Csp³-H), 1676 (C=O), 1633 (N=CH). ¹H NMR spectrum (400 MHz, DMSO-d₆), δ , ppm:

1.70-1.81 (1.71, 1.72, 1.77, 1.79, 1.81, m, 4H, CH₂), 2.74 (2.69, 2.71, 2.72, 2.76, 2.77, 2.79, dt, J = 25.4, 6.4 Hz, 4H, CH₂), 7.43 (7.43, 7.42, d, J = 3.7 Hz, 2H, ArH), 7.58 (7.57, 7.58, d, J = 2.1 Hz, 1H, ArH), 8.06 (8.05, 8.06, d, J = 1.9 Hz, 1H, ArH), 8.07 (8.07, 8.08, d, J = 2.1 Hz, 1H, ArH), 8.40 – 8.29 (8.13, 8.14, 8.15, 8.16, 8.16, m, 4H, ArH, NH, C=NH). ¹³C NMR spectrum (100,6 MHz, DMSO-d₆), δ, ppm: 22.55, 23.01, 25.54, 26.43, 113.55, 121.68, 124.97, 125.01, 125.11, 125.61, 130.39, 132.53, 135.22, 136.77, 143.81, 147.27, 150.54, 152.60, 154.59, 165.27.

Docking studies

As a result of a computational experiment, the most energetically favorable conformations of azomethine derivatives of 2-amino-4,5,6,7-tetrahydro-1-benzothiophene-3-carboxamide at the active site of AChE were selected.

According to the results of molecular docking, azomethine derivatives of 2-amino-4,5,6,7-tetrahydro-1-benzothiophene-3-carboxamide mainly form bonds with the following amino acid residues of the active site of AChE: Tyr 72, Asp 74, Trp 86, Gly 122, Tyr 124, Ser203, Trp 286, Val 294, Arg 296, Phe 295, Phe 297, Tyr 337, Phe 338, Tyr 341, Gly 446 and His 447.

In the table 1 are shown the minimum energies for the formation of ligand complexes with the active site of AChE and hydrogen bonds.

Compounds 3a, 3f, 3k, 3n, 3o and 3q form a hydrogen bond between the hydrogen atoms of the amino group and the amino acid Tyr 341, also with the same molecular group 3b makes a hydrogen bond with Tyr 124. Between the hydrogen atoms of the hydroxy group of the aryl fragments of the compounds 3c, 3d, 3e and 3g and Ser 293 the hydrogen bond can be formed. Compounds 3e and 3g can make a hydrogen bond between the oxygen atoms of their hydroxy groups with Arg 296. Molecular docking has shown that 3f forms two hydrogen bonds by its hydroxy groups with Arg 296. Carboxyl groups of 3c, 3e and 3g form a bond with Tyr 124 and 3h the same molecular group interacts with Ser 203. Methoxy group of compound 3m with its oxygen atoms can form a hydrogen bond with Arg 296. The compound 3l by the nitro group makes three hydrogen bonds with Gly 122, Ala 204 and His 447. The carboxyl group of 3r can form a hydrogen bond with Phe 295 as Donepezil. A hydrogen bond is formed between the hydroxyl group of the aryl

fragment of 3j, 3l and 3m and Asp 74, Tyr 124 and Phe 295, respectively. Azomethine 3p makes a hydrogen bond between the oxygen atom of the furan fragment and the amino acid Arg 296, and 3q similarly with Phe 295. Arg 296 of active site of AChE forms a hydrogen bond with the nitro group of 3s.

RMSD between the location of the Donepezil at the complex 2EY7 (X-ray diffraction analysis) and its location according to the molecular docking data is 0.44 angstrom.

Results of pharmacological study

The results of the anti-amyloid activity evaluation of the test substances are presented in Table 2.

The study showed that all the studied compounds are inferior in the severity of anti-amyloid activity to the referent. At the same time, the most significant amyloid-inhibiting properties among of test substances compounds under codes 3g; 3j; 3k and 3p were demonstrated.

The results of the anticholinesterase activity evaluation of the test substances are presented in Table 3

The analysis showed that the compounds have the highest anticholinesterase activity is 3d; 3e; 3f; 3m; 3n and 3o. It should be noted that the IC₅₀ of these compounds did not statistically differ from that of donepezil.

QSAR results

Antiamyloid action

Regression by Partial Least Squares (PLS)

For all 19 azomethine derivatives 797 descriptors were calculated using T.E.S.T. software. Selection of the most relevant descriptors for the regression model was based on forward selection procedure and hill climber optimization procedure. During selection we used model selection criteria cross-validation of the model (N=2). 8 most relevant descriptors were found (Table 4).

Also, correlation matrix between selected descriptors and activity was calculated (Table 5)

As a result the following model was obtained with R² = 0.9619. In purpose of estimation of prediction ability cross-validation was proceeded (N=1). Value of Q² = 0.8787.

Model:

$$\text{Activity} = 85.6759 * \text{knotpv} + 25.6375 * \text{BEHm8} + 150.337 * \text{BELe1} - 96.1271 * \text{MATS6p} - 81.3144 * \text{GATS7m} + 6.09769 * \text{GATS6v} - 19.6463 * \text{GATS1e} + 70.6769 * \text{GATS8p} - 224.532$$

Multiple Linear Regression (MLR)

We used the same 8 selected descriptors for MLR model. As a result, the following model was obtained with $R^2 = 0.9741$ In purpose of estimation of prediction ability cross-validation was proceeded (N=1). Value of $Q_2 = 0.9043$.

$$\text{Activity} = 101.402 * \text{knotpv} + 28.3653 * \text{BEHm8} + 103.448 * \text{BELe1} - 111.478 * \text{MATS6} - 81.8316 * \text{GATS7m} - 5.40736 * \text{GATS6v} - 34.6237 * \text{GATS1e} + 68.5012 * \text{GATS8} - 106.166$$

Artificial neural network (ANN)

On the basis of trial version of Molegro Data Modeller 7 we build the prediction model using ANN with the same 8 selected descriptors. ANN included: input layer: 9 neurons, hidden layer – 12 neurons and output layer = 1 neuron. As a result, the following model was obtained with $R^2 = 0.9926$ In purpose of estimation of prediction ability cross-validation was proceeded (N=1). Value of $Q_2 = 0.9923$.

Anticholinesterase action

For all 19 azomethine derivatives 797 descriptors were calculated using T.E.S.T. software. Selection of the most relevant descriptors for the regression model was based on forward selection procedure and hill climber optimization procedure. During selection we used model selection criteria cross-validation of the model (N=2). 6 most relevant descriptors were found (Table 6).

Also, correlation matrix between selected descriptors and activity was calculated (Table 7)

As a result, the following model was obtained with $R^2 = 0.9073$. In purpose of estimation of prediction ability cross-validation was proceeded (N=1). Value of $Q_2 = 0.7688$.

$$\text{Activity} = -4.33827 * \text{SaaS} + 0.356775 * \text{SCBO} - 50.9581 * \text{MATS5v} - 3.40811 * \text{GATS6m} + 14.193 * \text{GATS7v} - 9.82131 * \text{Br [aromatic attach]} - 15.6373$$

Regression by Partial Least Squares (PLS)

On the basis of forward selection procedure and hill climber optimization procedure we obtained 7 following the most relevant descriptors (Table 8).

Also, correlation matrix between selected descriptors and activity was calculated (Table 9)

As a result, the following model was obtained with $R^2 = 0,8648$. In purpose of estimation of prediction ability cross-validation was proceeded (N=1). Value of $Q_2 = 0,7400$.

$$\text{Activity} = -1.0081 * \text{Docking energy} - 17.4367 * \text{xp9} - 5.51545 * \text{SssO_acnt} - 15.3391 * \text{SHsNH2} + 24.4943 * \text{ATS7e} - 2.62567 * \text{GATS5e} - 4.87453 * \text{AC} + 3.37955$$

Discussion

AD is the most common form of dementia, the incidence of which is constantly increasing. Currently, two symptomatic treatment strategies are available for patients with AD: the use of anticholinesterase agents (donepezil, galantamine, rivastigmine) or NMDA receptor blockers (memantine). An alternative promising approach to AD therapy may be pathogenetic treatment aimed at suppressing amyloidogenesis as one of the main adverse prognostic events of AD [26]. At the moment, monoclonal antibodies – solanezumab, krenezumab, gantenerumabi adencanumab; BACE1 inhibitors – verubecystat and elenbekestat and a low-molecular-weight inhibitor of aggregation A β - sodium oligomannurate (GV-971) are at different stages of clinical trials [27, 28].

Considering the main directions of the development of new agents for the treatment of AD, namely pathogenetic agents based on the suppression of amyloidogenesis and symptomatic drugs that eliminate cholinergic deficiency, this study was conducted to study anticholinesterase and anti-amyloid activity, as well as quantitative structure-activity ratios for azomethine derivatives.

The results of molecular docking are in good line with the data of in vivo experiment to determine anticholinesterase activity, except for the compound 3s. The introduction of a vanillin series (3d - vanillin, 3e – isovaniline, 3f - ortho-vanillin) into the aryl fragment led to an increase in the ability of the studied compounds to inhibit the AChE. In doing so, of all the studied azomethine derivatives of 2-amino-4,5,6,7-tetrahydro-1-benzothiophene-3-carboxamide, the most active was the compound obtained as a result of the use of vanillin (3d). Compounds 3m, 3n and 3o in which the aryl fragment contains a bromine atom have also been shown to be effective for inhibiting acetylcholinesterase activity. The least active were azomethines obtained using aldehydes with furan heterocycles: 3p, 3q, 3r and 3s.

Figure 3 shows that the aryl fragment with methoxy and hydroxy groups of compounds 3d, 3e and 3f is located in the same direction of the active site of the enzyme as that of Donepezil, thereby

suggesting a close electrostatic interaction of the simulated compounds with the drug Donepezil. Thus, we suggest that the proposed design of AChE inhibitors is correct, as evidenced by data from *in vivo* experiments.

According to the data of the determination of anti-amyloid activity, the greatest activity was shown by compounds 3j and 3k in which the aryl part of the molecule contains a tert-butyl fragment. Also, 3g obtained using 2,4-dimethoxybenzaldehyde showed the amyloid-inhibiting property. The most active compound among the studied azomethine derivatives of 2-amino-4,5,6,7-tetrahydro-1-benzothiophene-3-carboxamide is 3p that includes an unsubstituted furan heterocycle in its structure. Thus, it is advisable to investigate the compounds 3g, 3j, 3k and 3p for the presence of cerebroprotective properties.

Value of R² and Q² for most QSAR models are greater than 0.86, which is a good result. We suppose that the QSAR models obtained can be used to further prediction anticholinesterase and anti-amyloid activity for structures with the same skeletal system.

Conclusion

In the course of the conducted studies, new azomethine derivatives of 2-amino-4,5,6,7-tetrahydro-1-benzothiophene-3-carboxamide were obtained, among which there are compounds that have shown high anticholinesterase and anti-amyloid activities. Azomethines with vanillin substituents showed the greatest anticholinesterase activity. The most significant amyloid-inhibiting properties have compounds with an unsubstituted furan heterocycle and containing a tert-butyl fragment in the aryl part of the molecule. The molecular mechanisms of anticholinesterase activity of the studied compounds have been studied by molecular docking method. QSAR models have been developed to predict anticholinesterase and anti-amyloid activity for structures having the same skeletal system. We consider it practicable in further study of these compounds in aspect of their possible use for the treatment of neurodegenerative diseases

Acknowledgments

The reported study was funded by RFBR, project number 20-315-90060

Conflict of interest: authors declare no conflict of interest

References

1. Z. Breijyeh, R. Karaman. Comprehensive Review on Alzheimer's Disease: Causes and Treatment. *Molecules*. 25 (2020), pp. 5789. doi:10.3390/molecules25245789.
2. J.L. Cummings, G. Tong, C. Ballard. Treatment Combinations for Alzheimer's Disease: Current and Future Pharmacotherapy Options. *J Alzheimers Dis*. 76 (2019), pp. 779-794. doi:10.3233/JAD-180766.
3. G. Esquerda-Canals, L. Montoliu-Gaya, J. Güell-Bosch, S. Villegas. Mouse Models of Alzheimer's Disease. *J Alzheimers Dis*. 57 (2017), pp. 1171-1183. doi:10.3233/JAD-170045.
4. G. Gallardo, D.M. Holtzman. Amyloid- β and Tau at the Crossroads of Alzheimer's Disease. *Adv Exp Med Biol*. 1184 (2019), pp. 187-203. doi:10.1007/978-981-32-9358-8_16.
5. L. Pinheiro, C. Faustino. Therapeutic Strategies Targeting Amyloid- β in Alzheimer's Disease. *Curr Alzheimer Res*. 16 (2019), pp. 418-452. doi:10.2174/1567205016666190321163438.
6. H. Amawi, N. Hussein, S.H.S. Boddu, C. Karthikeyan, F.E. Williams, C.R. Ashby, D. Raman, P. Trivedi, A.K. Tiwari. Novel Thienopyrimidine Derivative, RP-010, Induces β -Catenin Fragmentation and Is Efficacious against Prostate Cancer Cells. *Cancers*. 11 (2019), pp. 711. doi:10.3390/cancers11050711.
7. L. Ouyang, L. Zhang, J. Liu, L. Fu, D. Yao, Y. Zhao, S. Zhang, G. Wang, G. Liu. Discovery of a small-molecule bromodomain-containing protein 4 (BRD4) inhibitor that induces AMP-activated protein kinase-modulated autophagy-associated cell death in breast cancer. *Journal of Medicinal Chemistry*. 60 (2017), pp. 990-10012. doi:10.1021/acs.jmedchem.7b00275.
8. F. Ghayour, S. Mohammad, R. Mohammad, M. Ghashang. ZnO-CeO₂ nanocomposite: Efficient catalyst for the preparation of thieno[2,3-d]pyrimidin-4(3H)-one derivatives. *Main Group Metal Chemistry*. 41 (2018), pp. 21-26. doi:10.1515/mgmc-2017-0038.
9. S.G. Dzhavakhishvili, N.Yu. Gorobets, B.V. Paponov, V.I. Musatov, S.M. Desenko. Three possible products from the reactions of gewald's amide with

aromatic aldehydes. *Journal of Heterocyclic Chemistry*. 45 (2008), pp. 573-577. doi:10.1002/jhet.5570450243.

10. A. Missio, G. Bacher, A. Koul, A. Choidas. Axxima Pharmaceuticals AG., assignee. 4,5,6,7-Tetrahydrobenzo[B] thiophene derivatives and methods for medical intervention against mycobacterial infections. United States patent US 20090018149. 2009 Jan 15.

11. W. Zhu, H. Chen, Y. Wang, J. Wang, X. Peng, X. Chen, Y. Gao, C. Li, Y. He, J. Ai, M. Geng, M. Zheng, H. Liu. Design, Synthesis, and Pharmacological Evaluation of Novel Multisubstituted Pyridin-3-amine Derivatives as Multitargeted Protein Kinase Inhibitors for the Treatment of Non-Small Cell Lung Cancer. *Journal of Medicinal Chemistry*. 60 (2017), pp. 6018-6035. doi: 10.1021/acs.jmedchem.7b00076.

12. A.M.Sh. El-Sharief, A.A. Micky, N.A.M.M. Shmeiss, G. El-Gharieb. Synthesis and Reactions of Some Tetrahydrobenzothieno[2,3- d]Pyrimidine Derivatives with Biological Interest. Phosphorus, Sulfur and Silicon and the Related Elements. 178 (2003), pp. 439-451. doi: 10.1080/10426500307912.

13. S. Chigurupati, S.A. Shaikh, J.I Mohammad, K.K. Selvarajan, A.R. Nemala, C.H. Khaw, C.F. Teoh, T.H. Kee. In vitro antioxidant and in vivo antidepressant activity of green synthesized azomethine derivatives of cinnamaldehyde. *Indian J Pharmacol*. 49 (2017), pp. 229-235. doi:10.4103/ijp.IJP_293_16.

14. P.R. Nilkanth, S.K. Ghorai, A. Sathiyarayanan, K. Dhawale, T. Ahamad, M.B. Gawande, S.N. Shelke. Synthesis and Evaluation of Anticonvulsant Activity of Some Schiff Bases of 7-Amino-1,3-dihydro-2H-1,4-benzodiazepin-2-one. *Chem Biodivers*. 17 (2020), pp. e2000342. doi:10.1002/cbdv.202000342.

15. H. Todaka, M. Arikawa, T. Noguchi, A. Ichikawa. Donepezil, an anti-Alzheimer's disease drug, promotes differentiation and regeneration in injured skeletal muscle through the elevation of the expression of myogenic regulatory factors. *European Journal of Pharmacology*. 911 (2021), pp. 174528. doi:10.1016/j.ejphar.2021.174528.

16. A.J. Jung, E.J. Seong, P. Jun-Seong, C.S. Jae. Antidiabetic complications and anti-alzheimer activities of sophoflavescenol, a prenylated flavonol from *Sophora flavescens*, and its structure-activity

relationship. *Phytother. Res*. 25 (2011), pp. 709-715. doi:10.1002/ptr.3326.

17. H.A. Jung, B.S. Min, T. Yokozawa, J.H. Lee, Y.S. Kim, J.S. Choi. Anti-Alzheimer and Antioxidant Activities of Coptidis Rhizoma Alkaloids. *Biological & Pharmaceutical Bulletin*. 32 (2009), pp. 1433-1438. doi:10.1248/bpb.32.1433.

18. A. Homick, A. Lieb, N.P. Vo, J.M. Rollinger, H. Stuppner, H. Prast. The coumarin scopoletin potentiates acetylcholine release from synaptosomes, amplifies hippocampal long-term potentiation and ameliorates anticholinergic- and age-impaired memory. *Neuroscience*. 197 (2011), pp. 280-292. doi:10.1016/j.neuroscience.2011.09.006.

19. Z. Yang, Z. Song, W. Xue, J. Sheng, Z. Shu, Y. Shi, J. Liang, X. Yao. Synthesis and structure-activity relationship of nuciferine derivatives as potential acetylcholinesterase inhibitors. *Medicinal Chemistry Research*. 23 (2014), pp. 3178-3186. doi:10.1007/s00044-013-0905-9.

20. A.S. Chiriapkin, I.P. Kodonidi, M.V. Larsky. Targeted Synthesis and Analysis of Biologically Active Azomethine Derivatives of 2-amino-4,5,6,7-tetrahydro-1-benzothiophene-3-carboxamide. *Drug development & registration*. 10 (2021), pp. 25-31. doi: 10.33380/2305-2066-2021-10-2-25-31.

21. J. Cheung, M.J. Rudolph, F. Burshteyn, M.S. Cassidy, E.N. Gary, J. Love, M.C. Franklin, J.J. Height. Structures of Human Acetylcholinesterase in Complex with Pharmacologically Important Ligands. *J. Med. Chem*. 55 (2012), pp. 10282-10286, <https://doi.org/10.1021/jm300871x>.

22. J.T. Brian. Hyperchem, release 2: molecular modeling for the personal computer. *J. Chem. Inf. Comput. Sci*. 32 (1992), pp. 757-759.

23. G.M. Morris, R. Huey, W. Lindstrom, M.F. Sanner, R.K. Belew, D.S. Goodsell, et al. Autodock4 and AutodockTools4: Automated Docking with Selective Receptor Flexibility. *J Comput Chem*. 30 (2009), pp. 2785-2791. doi: 10.1002/jcc.21256.

24. W. Wang, C. Zhao, D. Zhu, G. Gong, W. Du. Inhibition of amyloid peptide fibril formation by gold-sulfur complexes. *J Inorg Biochem*. 171 (2017), pp. 1-9. doi:10.1016/j.jinorgbio.2017.02.021.

25. J. Jończyk, J. Godyń, E. Stawarska, B. Marak-Młodawska, M. Jelen, K. Pluta, B. Malawska. Dual Action of Dipyrithiazine and Quinobenzothiazine Derivatives-Anticancer and Cholinesterase-Inhibiting

Activity. *Molecules*. 25 (2020), pp. 2604. doi:10.3390/molecules25112604.

26. P. Lei, S. Ayton, A.I. Bush. The essential elements of Alzheimer's disease. *J Biol Chem*. 296 (2021), pp. 100105. doi:10.1074/jbc.REV120.008207.

27. L.K. Huang, S.P. Chao, C.J. Hu. Clinical trials of new drugs for Alzheimer disease. *J Biomed Sci*. 27 (2020), pp.18. doi:10.1186/s12929-019-0609-7.

28. M. Tolar, S. Abushakra S, J.A. Hey, A. Porsteinsson, M. Sabbagh. Aducanumab, gantenerumab, BAN2401, and ALZ-801-the first wave of amyloid-targeting drugs for Alzheimer's disease with potential for near term approval. *Alzheimers Res Ther*. 12 (2020), pp. 95. doi:10.1186/s13195-020-00663-w.

Figures

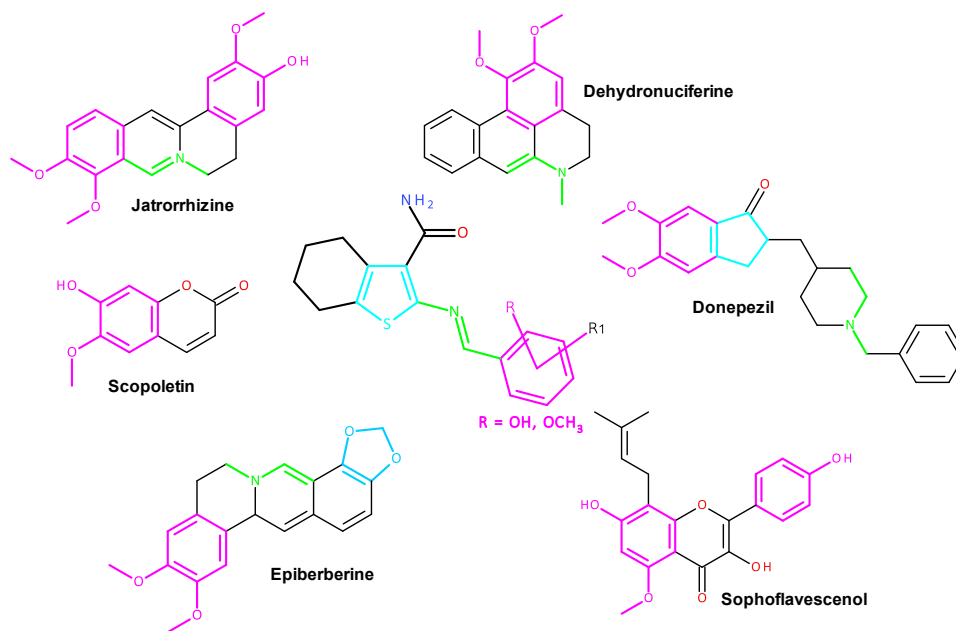


Figure 1. Design of AChE inhibitors

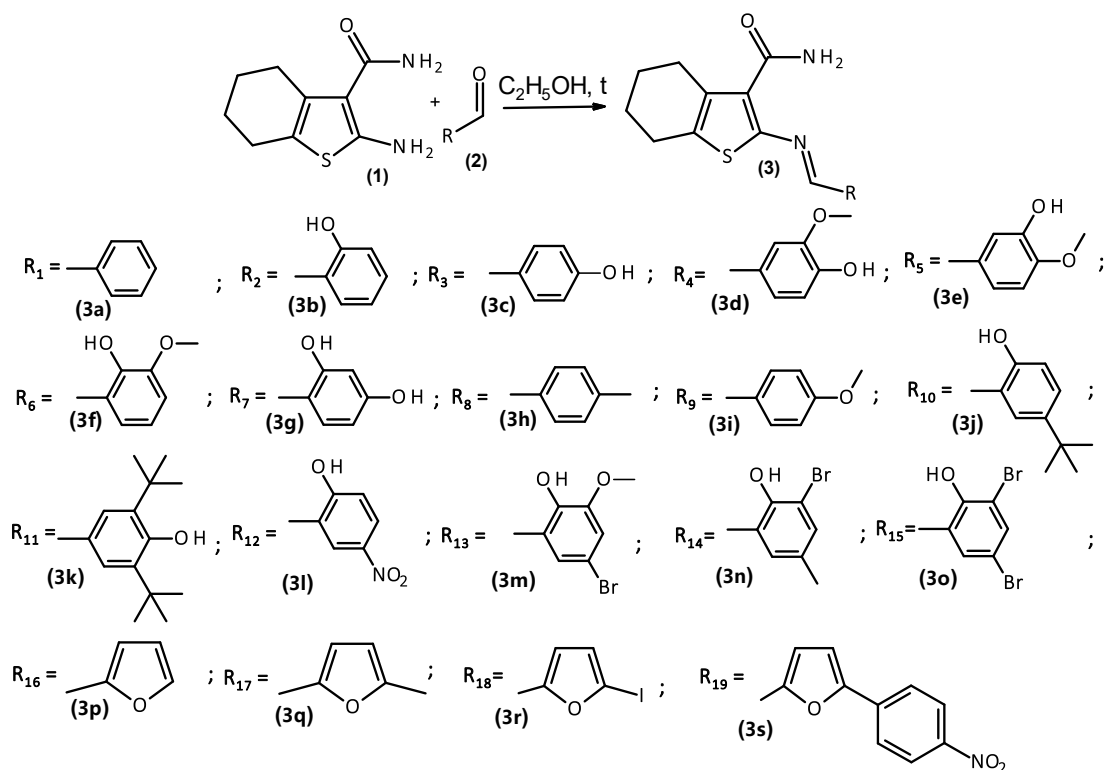


Figure 2. Synthesis of azomethine derivatives of 2-amino-4,5,6,7-tetrahydro-1-benzothiophene-3-carboxamide (3a-3s)

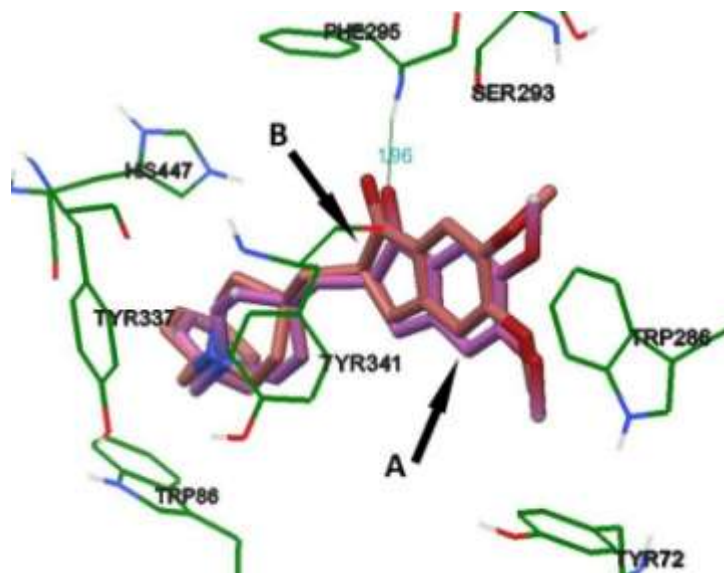


Figure 3. Location of Donepezil at active site of AChE. A - X-ray diffraction analysis (pink color), B - molecular docking (brown color)

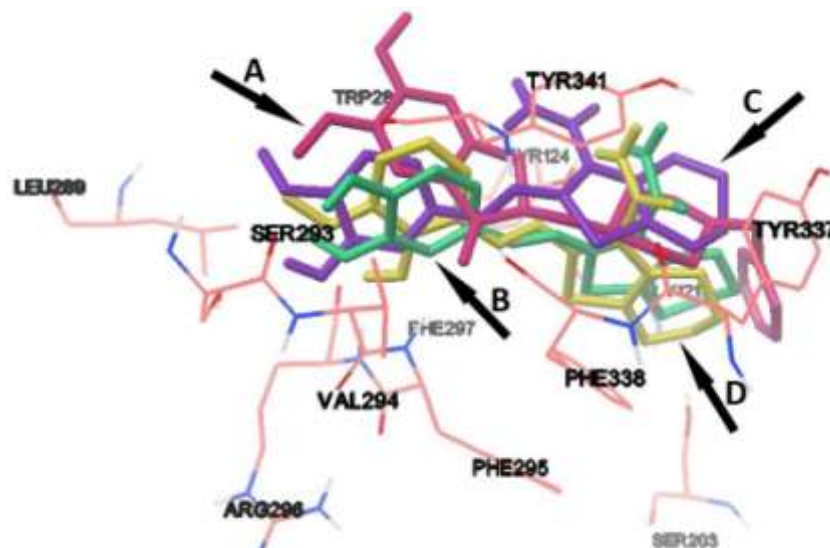


Figure 4. The location of Donepezil determined by X-ray diffraction analysis (A – red color) and location according to molecular docking: 3d (B - green color), 3e (C - purple color), 3f (D - yellow color)

Table 1. Results of molecular docking experiments for compounds 3a-3s and Donepezil and its hydrogen bonds

Compounds	AutoDock binding energy (kcal/mol)	Residue	Ligand atoms	Distance (Å)
3a	-9.02	Tyr 341	NH ₂	2.101
3b	-9.69	Tyr 124	NH ₂	2.206
3c	-9.28	Ser 293	OH	2.060
		Tyr 124	C=O	2.019
3d	-10.03	Ser 293	OH	2.007
		Tyr 341	NH ₂	1.948
3e	-10.30	Tyr 124	C=O	1.925
		Arg 296	OH	1.953
		Ser 293	OH	2.162

3f	-10.21	Tyr 341	NH ₂	2.231
		Arg 296	OH	1.857
		Arg 296	OH	2.072
3g	-9.72	Ser 293	OH	2.231
		Arg 296	OH	1.814
		Tyr 124	C=O	2.152
3h	-9.75	Ser 203	C=O	2.024
3i	-9.55	Tyr 124	NH ₂	2.133
3j	-10.70	Asp 74	OH	2.141
3k	-10.36	Tyr 341	NH ₂	2.192
3l	-9.87	Tyr 124	OH	2.143
		Gly 122	NO ₂	1.178
		Ala 204	NO ₂	2.088
		His 447	NO ₂	2.050
3m	-11.89	Tyr 341	NH ₂	2.211
		Phe 295	OH	2.152
		Arg 296	OCH ₃	2.223
3n	-11.25	Tyr 341	NH ₂	2.212
3o	-11.64	Tyr 341	NH ₂	2.170
3p	-8.81	Arg 296	FuranO	1.849
3q	-9.02	Tyr 341	NH ₂	2.232
		Phe 295	FuranO	2.146
3r	-9.57	Phe 295	C=O	2.074
3s	-11.50	Arg 296	NO ₂	1.905

Donepezil	-11.89	Phe 295	C=Q	1.770
-----------	--------	------------	-----	-------

Table 2. The effect of the studied compounds and GV-971 on the aggregation of amyloid particles

Compounds	% of inhibition
3a	21,3±0,9*
3b	56,3±0,4*
3c	59,8±0,3*
3d	30,1±0,5*
3e	27,6±0,8*
3f	29,4±0,2*
3g	69,5±0,1*
3h	41,2±0,5*
3i	40,9±0,6*
3j	70,2±0,5*
3k	71,3±0,9*
3l	20,1±0,3*
3m	38,7±0,3*
3n	30,4±0,7*
3o	29,7±0,7*
3p	74,6±0,5*
3q	25,9±0,2*
3r	48,3±0,9*
3s	50,4±0,5*
GV-971	89,3±0,5

Note: *- statistically significant relative GV-971 (ANOVA with the Tukey post-test, $p < 0,05$)

Table 3. The effect of the studied compounds and Donepezil on acetylcholinesterase activity

Compounds	IC ₅₀ , mg/ml
3a	12,2±0,14*
3b	16±0,99*
3c	8,2±0,35*
3d	3±0,01
3e	4,3±0,47
3f	3,9±0,59
3g	9,9±0,61*
3h	10,3±0,93*
3i	8,1±0,2*
3j	11,8±0,24*
3k	6,8±0,97*
3l	11,7±0,48*
3m	5,7±0,43
3n	6,3±0,95
3o	6,1±0,48
3p	15,7±0,64*
3q	14,7±0,66*
3r	12,6±0,12*
3s	14,9±0,23*
Donepezil	2,5±0,58

Note: *- statistically significant relative Donepezil (ANOVA with the Tukey post-test, p<0,05)

Table 4. Activity and descriptors values

Activity	knotpv	BEHm ₈	BELe1	MATS6	GATS7 _m	GATS6 _v	GATS1 _e	GATS8
21,3	-0,9	2,4	1,9	0,0	0,6	0,9	0,6	0,6
56,3	-1,0	2,5	1,9	-0,3	0,6	1,1	0,6	0,6
59,8	-0,9	2,5	1,9	0,2	0,6	0,6	0,6	1,2
30,1	-1,0	2,5	1,9	0,1	0,9	0,7	0,8	1,3
27,6	-1,0	2,7	1,9	0,1	0,9	0,6	0,8	1,3
29,4	-1,1	2,7	1,9	-0,3	0,9	1,0	0,8	0,9
69,5	-1,0	2,6	1,9	-0,1	0,6	0,8	0,6	1,1
41,2	-0,9	2,6	1,9	0,0	0,6	1,0	0,6	0,8
40,9	-1,0	2,6	1,9	0,2	0,6	0,6	0,8	1,2
70,2	-0,9	2,6	1,9	-0,3	1,0	1,7	0,6	1,0
71,3	-0,6	2,7	2,0	0,1	1,5	0,8	0,6	1,6
20,1	-1,1	2,5	1,9	0,2	1,0	0,7	0,5	1,4
38,7	-1,1	2,7	1,9	-0,2	0,7	0,9	0,8	0,9
30,4	-1,2	2,7	1,9	-0,2	0,7	0,9	0,6	0,8
29,7	-1,2	2,7	1,8	-0,2	0,7	0,8	0,6	0,9
74,6	-0,9	2,2	1,8	-0,1	0,1	1,3	0,8	0,9
25,9	-0,9	2,3	1,8	-0,1	0,6	1,2	0,8	0,8
48,3	-0,9	2,3	1,8	0,0	0,9	0,8	0,8	1,6
50,4	-1,1	2,7	1,9	0,0	0,6	1,1	0,6	1,1

Table 5. Correlation matrix between for selected descriptors (MLR, PLS, ANN)

	Activi	knotpv	BEHm8	BELe1	MATS6	GATS7m	GATS6v	GATS1e	GATS8
Activity		0.294	0.021	0.031	0.045	0.004	0.141	0.011	0.049
knotpv	0.294		0.093	0.052	0.042	0.120	0.044	0.000	0.130
BEHm8	0.021	0.093		0.572	0.011	0.248	0.067	0.124	0.007
BELe1	0.031	0.052	0.572		0.002	0.404	0.003	0.403	0.026
MATS6	0.045	0.042	0.011	0.002		0.011	0.479	0.000	0.370
GATS7m	0.004	0.120	0.248	0.404	0.011		0.036	0.056	0.335
GATS6v	0.141	0.044	0.067	0.003	0.479	0.036		0.000	0.217
GATS1e	0.011	0.000	0.124	0.403	0.000	0.056	0.000		0.002
GATS8	0.049	0.130	0.007	0.026	0.370	0.335	0.217	0.002	

Table 6. Activity and descriptors values

Activity	SaaS	SCBO	MATS5 _v	GATS6 _m	GATS7 _v	-Br [aromatic attach]
12,2	1,6	29,5	-0,3	1,1	0,9	0,0
16,0	1,5	30,5	-0,2	1,4	1,2	0,0
8,2	1,6	30,5	-0,2	1,1	0,8	0,0
3,0	1,5	32,5	-0,1	1,1	1,0	0,0
4,3	1,5	32,5	-0,1	1,1	1,1	0,0
3,9	1,5	32,5	-0,1	1,4	1,2	0,0
9,9	1,5	31,5	-0,2	1,3	1,1	0,0
10,3	1,6	30,5	-0,2	1,1	0,9	0,0
8,1	1,6	31,5	-0,2	1,1	0,9	0,0
11,8	1,5	34,5	-0,2	1,3	1,1	0,0
6,8	1,6	38,5	-0,1	0,8	0,8	0,0
11,7	1,4	34,5	-0,2	1,2	1,1	0,0
5,7	1,5	33,5	-0,3	0,6	1,0	1,0
6,3	1,5	32,5	-0,3	0,6	0,9	1,0
6,1	1,5	32,5	-0,5	0,6	0,9	2,0
15,7	1,6	28,0	-0,4	1,1	0,9	0,0
14,7	1,6	29,0	-0,4	1,1	0,8	0,0
12,6	1,6	29,0	-0,3	0,6	0,8	0,0
14,9	1,5	42,0	-0,3	1,1	0,8	0,0

Table 7. Correlation matrix between for selected descriptors (MLR)

	Activi	SaaS	SCBO	MATS5v	GATS6m	GATS7v	-Br [arom.]
Activity		0.013	0.020	0.231	0.091	0.049	0.124
SaaS	0.013		0.133	0.018	0.017	0.225	0.044
SCBO	0.020	0.133		0.072	0.007	0.005	0.002
MATS5v	0.231	0.018	0.072		0.160	0.242	0.312
GATS6m	0.091	0.017	0.007	0.160		0.289	0.460
GATS7v	0.049	0.225	0.005	0.242	0.289		0.011
-Br [aromatic attach]	0.124	0.044	0.002	0.312	0.460	0.011	

Table 8. Activity and descriptors values

Activity	Docking energy	xp9	SssO_act	SHsNH ₂	ATS7e	GATS5e	AC
12,2	-9,0	1,0	0,0	1,7	3,0	1,6	5,0
16,0	-9,7	1,0	0,0	1,8	3,2	1,2	6,0
8,2	-9,3	1,0	0,0	1,7	3,1	1,2	6,0
3,0	-10,0	1,1	1,0	1,8	3,2	0,9	7,0
4,3	-10,3	1,1	1,0	1,8	3,2	1,0	7,0
3,9	-10,2	1,1	1,0	1,8	3,3	0,9	7,0
9,9	-9,7	1,0	0,0	1,8	3,2	1,1	7,0
10,3	-9,8	1,0	0,0	1,7	3,0	1,6	6,0
8,1	-9,6	1,1	1,0	1,7	3,1	1,2	6,0
11,8	-10,7	1,2	0,0	1,8	3,4	1,3	7,0
6,8	-10,4	1,3	0,0	1,8	3,5	0,9	8,0
11,7	-9,9	1,1	0,0	1,8	3,4	1,2	7,0
5,7	-11,9	1,2	1,0	1,8	3,4	0,9	8,0
6,3	-11,3	1,2	0,0	1,8	3,4	1,4	8,0
6,1	-8,8	1,2	0,0	1,8	3,4	1,1	8,0
15,7	-9,0	0,9	0,0	1,7	3,0	1,3	5,0
14,7	-9,6	1,0	0,0	1,7	3,1	1,4	6,0
12,6	-11,5	1,0	0,0	1,7	3,1	1,4	6,0
14,9	-11,9	1,6	0,0	1,8	3,6	1,1	6,0

Table 9. Correlation matrix between for selected descriptors (PLS)

	Activi	Docking	xp9	SssO_ac	SHsNH2	ATS7e	GATS5e	AC
Activity		0.009	0.019	0.458	0.055	0.091	0.345	0.460
Docking energy	0.009		0.368	0.031	0.262	0.340	0.090	0.133
xp9	0.019	0.368		0.002	0.580	0.790	0.245	0.190
SssO_acnt	0.458	0.031	0.002		0.036	0.011	0.350	0.056
SHsNH2	0.055	0.262	0.580	0.036		0.784	0.473	0.357
ATS7e	0.091	0.340	0.790	0.011	0.784		0.410	0.539
GATS5e	0.345	0.090	0.245	0.350	0.473	0.410		0.391
AC	0.460	0.133	0.190	0.056	0.357	0.539	0.391	